CORRELATING AERIAL AND GROUND-BASED HYPERSPECTRAL DATA WITH MICROBIAL COMPOSITION AND DIVERSITY IN A MARS ANALOG HYDROTHERMAL SYSTEM IN ICELAND. U. Basu[1], P. Schroedl[2], M. S. Phillips[3], J. E. Moersch[1], K. Warren[3], Y. Maierhaba[3], C. W. Hamilton[4]. [1]Dept of Earth and Planetary Sciences, Univ. of Tennessee, Knoxville, TN. [2]Department of Biology, Boston University. [3]The Johns Hopkins University Applied Physics Laboratory. [4]Lunar and Planetary Laboratory, Univ. of Arizona, Tucson, AZ

Introduction: Advances in our understanding of Mars' environmental history have led to a shift in NASA's overarching strategy for Mars exploration from "follow the water" to "seek signs of life"[1]. Now that the evidence for extensive, ancient water on Mars has been established in multiple localities[2], attention is being focused on identifying specific sites within these localities that are most likely to have hosted and preserved evidence for life at a scale that is relevant for sample collection[3]. Determining the optimal measurement approaches for finding such sites is an important component to this new strategy.

Hydrothermal systems have been associated with the development of early life on Earth and are identified as high priority targets of interest on Mars that could host evidence of life[4]. Geochemical conditions at terrestrial hydrothermal systems influence which chemical species are present for microbial ecological functions and metabolisms[5]. Temperature and pH gradients in such systems have been shown to correlate with changes in microbial communities[6,7]. These systems may preserve evidence for life or at least habitable niches[8].

The Námafjall geothermal area is a part of the larger Krafla geothermal system in north-central Iceland. Námafjall lies on the east side of Lake Myvatn (Figure 1), astride the eastern part of the main fissure swarm with which the Krafla central volcano is associated[9,10]. This environment has been identified as a Mars analog site[11], as early Mars would also have had geothermally active areas with water heating from below and rising to the surface. We sampled and took drone and ground-based hyperspectral scenes in an isolated location away from tourists and general foot traffic.

Goal: Here we describe our preliminary results in evaluating the utility of visible to short-wave infrared hyperspectral images collected from ground-based and aerial platforms for locating sites of high astrobiological relevance within the hydrothermal fumarolic system at Námafjall. We conduct this evaluation by looking for correlations between spectral signatures in the hyperspectral images and variations in the microbial community composition and diversity within the site.

Methods: A hyperspectral camera is a device that collects light in contiguous, narrow spectral bands across a region of the electromagnetic spectrum. Whereas a traditional camera only collects data in three bands (namely red, green, and blue), a hyperspectral camera may take data in hundreds of wavelength bands. A hyperspectral cube is a three-dimensional array in which two axes are orthogonal spatial dimensions along the ground and the third axis is in the spectral dimension. Every pixel in a processed hyperspectral cube contains a reflectance spectrum for the corresponding location in the scene.

Fig. 1: Map showing the study location in north Iceland[2].

We employed a HySpex hyperspectral camera made by Norsk Elektro Optikk. The Mjolnir VS-620 acquires concurrent visual-near infrared (VNIR; 400–1000 nm) data and short-wave infrared (SWIR; 970–2500 nm) data from two camera subsystems[13] while affixed to a drone or a scan platform on a tripod. Hyperspectral instruments are typically quite large and heavy and therefore are usually affixed to aircraft or satellites, forcing spatial resolution to be relatively poor. However, the relative compactness and low mass of our device allow for deployment on drones, producing hyperspectral images at centimeter, if not millimeter spatial resolution.

We have identified three different fumarole deposits in Námafjall that exhibited varying levels of activity. One was identified to be *partially active* with some steam coming out from it at intermittent times throughout the day, another fumarole was identified to be *inactive* as there seemed to be no steam coming out of it, and the last fumarole was *very active*, producing profuse amounts of steam. Aluminum stakes were placed as markers at regular intervals along transects radiating out from the fumaroles. Samples were acquired from these marked areas using 70% ethanol and flame-sterilized rock hammers and stored in whirl-paks on ice. Temperature and pH were measured in conjunction at the markers along the sampled transects. Genetic materials were extracted from frozen samples to assess changes in regolith-hosted community composition and diversity along the transects. The samples exhibited *in-situ* temperatures of 23.0 – 98.4 °C, acidic pH (2–3), and low genetic content (200–2000 ng/mL) in subsample extractions (~250 mg).

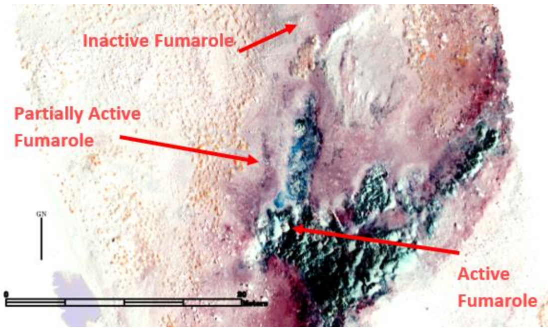

Fig. 2: A VNIR hyperspectral mosaic from two hyperspectral scenes acquired by a drone with a spatial resolution of ~2 cm/pixel at Námafjall. Indicated are the hydrothermal fumarole deposits from which biosignature samples were acquired.

An aerial hyperspectral drone scene and ground-based hyperspectral scenes were acquired with the aluminum marker stakes present in the images, allowing for easy cross-identification of regolith sample locations so that a comparison between the biological survey results and hyperspectral data could be made.

Post-processing and Preliminary Results: Hyperspectral data from the drone initially come in an array of raw data numbers that are proportional to the amount of radiance received by the detector. These data are then radiometrically calibrated, which converts the raw numbers recorded by the instrument into spectral radiance [W/m^2/sr/µm]. The drone's path is recorded using a GNSS receiver to provide accurate Real-Time Kinematic position data. These data are then georeferenced, where every pixel of data acquired by the camera is assigned a geographic coordinate.

Georectification corrects the images for spatial distortions. At this point, the VNIR and SWIR hyperspectral cubes are merged along the spectral dimension into a single hyperspectral cube that spans a spectral range of 400–2500 nm. This process is repeated for all flight lines and the scenes are mosaicked to produce a single composite hyperspectral image such as the one presented in Fig. 2. The composite hyperspectral image is then empirically calibrated using three in-scene Spectralon calibration targets (R = 0.05, 0.50, and 0.98) to convert the data into reflectance and to correct for any atmospheric effects.

The Minimum Noise Fraction (MNF) transform is used to determine the inherent dimensionality of image data, to segregate and equalize the noise in the data, and to reduce the computational requirements for subsequent processing. The resulting bands of the MNF-transformed data are ranked with the largest amount of spectral variance in the first few bands and decreasing spectral variance with increasing band number until only noise and spatially incoherent images remain. The number of significant MNF bands can roughly indicate the number of intrinsic spectral endmembers contained in the image.

Conclusion: Developing these color maps and further extractions on the remaining regolith samples may help reveal spectral signatures that correlate with microbial community composition and diversity in harsh hydrothermal conditions. Such correlations could exist either because of direct spectral detection of biosignatures, or more likely because certain mineral compositions are found in association with different microbial communities at these sites. If such correlations are found, it would suggest that high spatial resolution hyperspectral imaging, either from drones or ground-based platforms, could have value for future Mars missions with astrobiological goals.

References: [1] The Mars Exploration Program NASA. [2] Nazari-Sharabian, M., et al. (2020). *Galaxies*, *8*(2), 40. [3] Warren-Rhodes, et al. in press for Nature Astro., 2022. [4] Duhamel, S., et al. (2022). *Astrobio.*, *22*(10), 1176-1198. [5] Lindsay M. R., et al. (2018). *Geobio.*, *16*(6), 674–692. [6] Colman, D. R., et al. (2019). *Astrobio.*, *19*(12), 1505–1522. [7] Crognale, S., et al. (2022). *FEMS Microbio. Ecology*, *98*(10). [8] Havig, J. R., et al (2021). *Astrobio.*, *21*(12), 1526–1546. [9] Gudmundsson, B. T. & Arnórsson, S. (2002). *Geothermics*, *31*(2), 195-243. [10] Sæmundsson, K. (1991). Geol. of the Krafla system. *The Nat. Hist. of Lake Myvatn*, 24-95. [11] Mínguez, H. A., et al. (2011). *Revista de la Soc. Española de Mineralogía*, *15*, 25–26. [12] Ende, J. J., & Szynkiewicz, A. (2021). *Icarus*, *368*, 114608. [13] J. Moersch, et al., LPSC 2020, Abstract #1865

Acknowledgements: Funding was provided by NASA PSTAR Grant # 80NSSC21K0011.

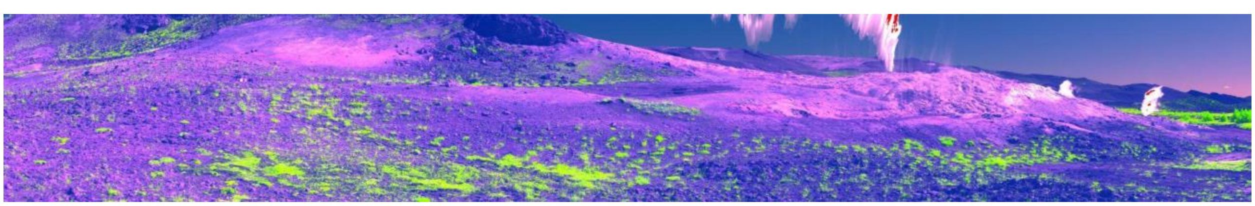

Fig 3: A Minimum Noise Fraction (MNF) transformation image showing the 2nd, 3rd, and 5th largest MNF bands, indicating higher data variance in the transformed band, as red, green, and blue respectively in the image.